



# Microstructure Investigation of Activated Carbon Prepared from Potato Peel

<sup>1,2</sup>Ammar Mukhlif Jasim\*, <sup>1</sup>Nathera Abass Ali

<sup>1</sup>Department of Physics, College of Science, University of Baghdad – Iraq

<sup>2</sup>Department of Applied Sciences, University of Technology – Iraq

## Article information

### Article history:

Received: November, 19, 2022

Accepted: April, 17, 2023

Available online: June, 10, 2023

### Keywords:

KOH,  
Carbon dioxide,  
Active Carbon

### \*Corresponding Author:

Ammar Mukhlif Jasim

[amar.moukhalaf1104a@sc.uobaghdad.edu.iq](mailto:amar.moukhalaf1104a@sc.uobaghdad.edu.iq)

## Abstract

This research investigates how activated carbon (AC) was synthesized from potato peel waste (PPW). Different ACs were synthesized under the atmosphere's conditions during carbonation via two activation methods: first, chemical activation, and second, carbon dioxide-physical activation. The influence of the drying period on the preparation of the precursor and the methods of activation were investigated. The specific surface area and pore volume of the activated carbon were estimated using the Brunauer–Emmett–Teller method. The AC produced using physical activation had a surface area as high as 1210 m<sup>2</sup>/g with a pore volume of 0.37 cm<sup>3</sup>/g, whereas the chemical activation had a surface area of 1210 m<sup>2</sup>/g with a pore volume of 0.34 cm<sup>3</sup>/g. The main aim of this research is to produce activated carbon from natural materials and to prepare and characterize the elemental analysis, surface area, and morphological properties of ACs from potato peel waste using potassium hydroxide (KOH) AC-PPK and Carbon dioxide (CO<sub>2</sub>) AC-PPC as activating agents. X-ray diffraction analysis showed the degree of crystallinity to be 35.03% in the case of AC-PPK, and AC-PPC showed a crystallinity of 35.46%. In both methods, the results showed that the crystallographic structure revealed that all the synthesized AC took on an amorphous state with low crystallinity. The atomic force microscopy (AFM) image of AC shows the presence of nanotips on the surface and shows that the maximum height was 1396 nm and 778 nm. The outer surfaces are full of cavities and highly irregular as a result of activation. The morphological analysis of the precursors was determined by scanning electron microscopy. The external surfaces are full of cavities and quite irregular as a result of activation. Also, activated carbon prepared from potato peel waste is a low-cost and effective adsorbent when compared with several activated carbon sources.

DOI: [10.53293/jasn.2023.5760.1196](https://doi.org/10.53293/jasn.2023.5760.1196), Department of Applied Sciences, University of Technology

This is an open access article under the CC BY 4.0 License.

## 1. Introduction

Activated carbon adsorbents have found numerous and diverse applications in recent times, frequently as a result of both a well-created polydisperse permeable structure with a measure of dispersion favorable for atomic sorption

and a large inside surface region [1]. Any carbonaceous solid, natural or synthetic, is a carbon precursor [2]. In most cases, waste material is used as a precursor due to its availability, cheap price, and continuous need for recycling waste [3]. Examples of carbon precursors are; agricultural residues, forestry wastes, sewage sludge, used tires, and waste plastics [4]. The carbon precursor consists of (i) graphitic fabric (carbon), which is the main portion of the precursor, and (ii) impurities, which are non-graphitic fabrics such as inorganic matter (salts) [5]. As a result, it is critical to select appropriate precursor materials with high density and rising hardness, but the low inorganic structure, to produce a kindly AC [6]. Non-porous materials exist within the inorganic material structures; therefore, the adsorption ability will be reduced, in amount and accessibility. The cost of crude materials influences the ultimate price fetched. Particularly with significant masslessness in all activation treatments [7]. So, materials with a high carbon content are favorable for the generation of enacted carbon, as these materials don't require costly forms to deliver the enacted carbon [8]. Generally, brown wood, cellulosic materials, and a little bit of polymer are used as tall carbon roots to produce AC materials. [9]. Because of its accessibility and high content of cellulose, lignin, and hemicellulose, wood is the most commonly used fabric in actuated carbon generation. [10]. There has been surprising intrigue within the generation of AC due to its absorptive, natural, warm, electrical, and mechanical attributes [11]. Previous research on features such as porous structure and adsorption gain ability discovered that AC has a mechanical material structure [12]. As of now, there have been numerous studies on the auxiliary properties of active carbon. Ahmed I. Osman [13] studied activated carbon synthesized from potato peel waste (PPW) using XRD analysis and SEM, and the diffraction lines that refer to crystalline and amorphous cellulose phases constructed the precursor PPW. The fabric's surface region, pore volume, and included esteem were compared with the parameters of the precursor potato peel. The use of potato peels as feedstock not only results in a run of unused enacted carbon materials, but it may also be risky in terms of accessibility and feasibility [14]. The goal of this study is to plan and characterize the basic investigation, surface region, and morphological properties of ACs derived from potato peel waste (PPW). Chemical activation involves pyrolysis. However, in this case, the biomass is first activated with chemical agents such as  $H_3PO_4$ ,  $ZnCl_2$ , or  $KOH$  [15]. These are the most common activators.  $ZnCl_2$  is considered to be the most expensive activating agent, while the cheapest activating agent is  $KOH$ , and it has been extensively used in this investigation [13]. The pyrolysis of the activated biomass then occurs at much lower temperatures than that of the physical activation, typically at temperatures of approximately  $500\text{ }^\circ\text{C}$  [16]. Physical activations involve pyrolysis of the source material at  $600\text{--}800\text{ }^\circ\text{C}$  to produce charcoal [17]. Analysts detailed the impact of interfacial structure on the interfacial properties between actuated carbon fillers and the natural matrix of composites. Regardless, the high surface region and porosity are required for activated carbon [18].

## 2. Experimental Procedure

### 2.1 Preparing Precursor

Potato peel waste (PPW) has been used as the carbon precursor in this study. They do a preparatory washing well several times before the process of obtaining potato peels to remove mud or impurities using distilled water. The precursor sample dried in the environment at around  $100\text{ }^\circ\text{C}$ , as shown in Table 1. The drying was carried out during different periods to study the effect of this on the spectroscopic PPW. Where  $W_0$  and  $W$  it indicated, they indicate the weight before and after the drying process, respectively.

**Table 1:** Potato peel waste precursors weights before and after different drying periods.

Samples	$W_0$	$W$	Dried Time
PPW1	52.7g	11.6g	12 Hr
PPW2	51.3g	10.4g	24 Hr
PPW3	52.1g	8.5g	48 Hr

### 2.2 Synthesis of Activated Carbons

Herein, activated carbons from PPW have been synthesized by chemical activation with  $KOH$  (86%), obtained from Riedel-de Haën AG, and physical activation with  $CO_2$ . The washing process for these resulting carbons to remove the residuals of reactants and inorganic matter (ash) from the precursor makes the processing time- and energy-consuming, expensive, and environmentally unfriendly [18]. On the other hand, physical activation presents some disadvantages: the ACs are obtained in two steps, with higher temperatures of activation and poorer control of the porosity [19].

### 2.3 Chemical Activation

Chemical Impregnation Step: The chemical agent KOH was used for impregnating potato peel waste (PPW). This is done by mixing PPWs, as shown in Table 1, with potassium hydroxide and deionized water at a ratio of 30%, as shown in the table below. At a temperature of 100 °C for a period of one hour, the blend was stirred and left at room temperature for 24 hours to dry, as shown in Table 2. The samples were assigned as PPK

**Table 2:** Shown the impregnation PPW in KOH.

Sample	PPW	KOH	Deionized water	Time Impregnation
PPK1	1.12g	0.338g	5ml	24Hr
PPK2	1.11g	0.320g	5ml	24Hr
PPK3	1.12g	0.389g	5ml	24Hr

Activation has been achieved by heating the PPKs in an oven (MTI Corp.) at around  $500 \pm 5$  °C (with a heating rate of 5 °C per minute for 30 minutes). Then the samples have been left to cool at room temperature, during the activation phase, impurities may be generated and must be removed by washing with deionized water and HCL with a ratio of 1:1 several times to get rid of any traces of activation and to neutralize the pH. The clean activated carbon was dried at  $100 \pm 5$  °C for 24 hours before being saved in containers for further study, as shown in Figure 1.



**Figure 1:** PPK Chemical Activation Samples.

### 2.4 Physical Activation

Physical activation is a two-step process in which the Potato Peel Waste (PPW) is first carbonized at 600 °C, followed by activation of the resulting char with oxidant gases such as CO<sub>2</sub>. The samples were assigned as PPC in Table 3.

**Table 3:** The physical activation samples of PPC.

Samples	PPC	GAS	Temp	Time
PPC1	1.10g	CO <sub>2</sub>	600°C	30min
PPC2	1.09g	CO <sub>2</sub>	600°C	60min
PPC3	1.06g	CO <sub>2</sub>	600°C	90min

Carbonization step; in this study, precursor PPWs were used for carbonization experiments in the environment's atmosphere, as shown in Table 1. Table 3 shows the ratio of PPCs after the carbonization process.

The 80 cm quartz tube with a 40 mm diameter is placed horizontally in the furnace with a CO<sub>2</sub> (1 mL/min) flow [19]. A small crucible (10 mm in diameter) was used and inserted into the tube at a temperature of  $600 \pm 5$  °C with a heating rate of 5 °C per minute to facilitate the handling of the material (powder) after the activation process. Then the PPCs were left to cool at room temperature and saved in containers for study, as shown below in Figure

2.



**Figure 2:** The PPW samples coal under a 600 °C tube furnace.

## 2.5 Material Characterization

The X-ray diffraction (XRD) technique has been used to determine the crystallographic structure of PPW, PPK, and PPC. The analysis was carried out using XRD SSC with a copper K- X-ray tube (wavelength @ 0.15406) and a power source of 30KV/20mA. The data on diffracted radiation were obtained using a variable angle ( $2\theta$ ) range of 10 to 80. The degree of crystallinity of the precursor was estimated as follows [20]:

$$\% X_c = \frac{A_c}{(A_c + A_a)} \times 100 \quad (1)$$

Where: % Xc refers to a degree of crystallinity, Ac refers to the crystallized area on the X-ray diffractogram; and Aa refers to the amorphous area on the X-ray diffractogram.

AFM estimations of arranged samples of potato peels for prepared activated carbon with various connected conditions were performed with an AFM (NaiioAFM Naosurf Switzerland) to get a clear quantitative picture of grain size and surface harshness for precursors PPWs, PPKs, and PPCs. The morphology studies of the precursors were conducted using the ultra-high resolution Field Emission Scanning Electron Microscope (FE-SEM) images collected on the ARYA Electron Optic MIRA3 FE-SEM Microscope. The precursors were mounted onto an SEM holder with double-sided electrically-conducting carbon adhesive tabs to block the surface of the specimens when exposed to the electron beam. The chambers use a 5-axis, fully motorized, compucentric stage that provides superior specimen handling and has an ideal geometry with ultra-high resolution at low beam energy: 1 nm at 1 keV and 0.7 nm at 15 keV.

## 3. Results and Discussion

### 3.1 Characterization of Precursor

As shown in Figure 3, the Potato Peel Waste (PPW) was obtained from a local market throughout the experiments. The crystallographic structure, grain size, surface harshness, and morphological and elemental information of the potato peel were explored through AFM, XRD, and FE-SEM, analysis to prepare activation carbon.



**Figure 3:** Prepare activation carbon precursor.

The X-ray diffraction patterns (XRD) of the three precursors (PPW1, PPW2, and PPW3), the product of activation carbon AC using the chemical process (PPK1, PPK2, and PPK3), and via physical activation (PPC1, PPC2, and PPC3), were recorded as shown in Figures 4-6 to see the nanoparticle measure and crystalline and undefined

materials. The presence of a broad diffraction foundation and the absence of peaks for the precursors The influence of the drying period on the crystallographic structure The influence of the drying period on the crystallographic structure was revealed as the amorphous state with low crystallinity for the synthesized AC (PPK and PPC), as shown in Figures 5–6.

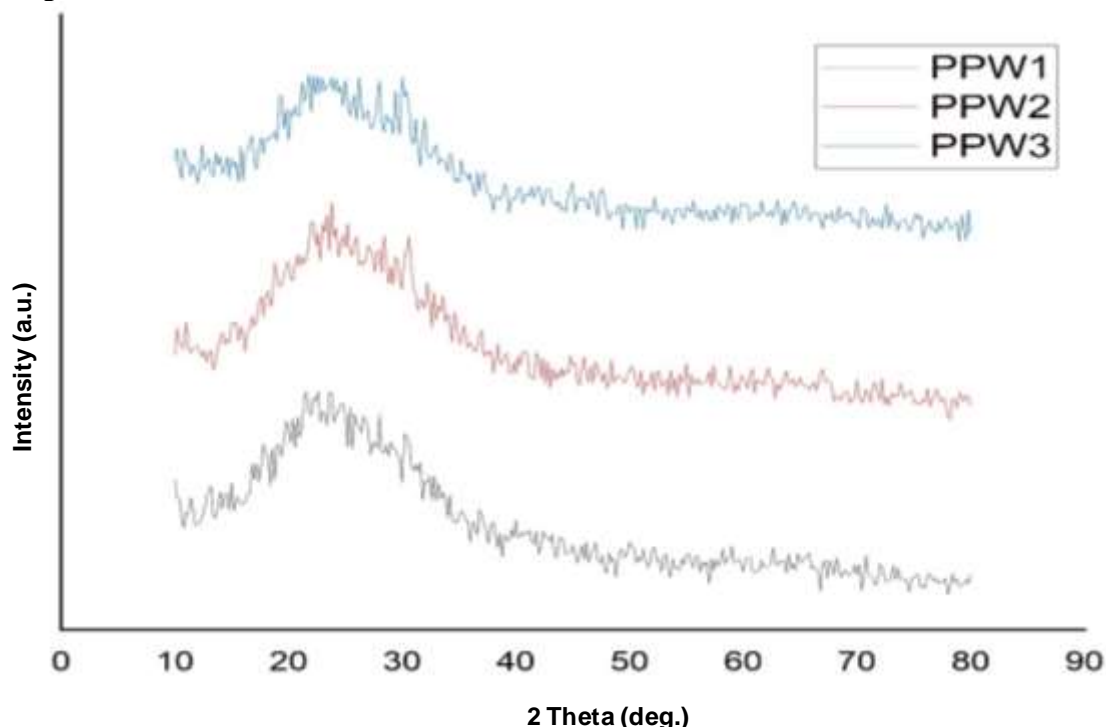


**Figure 4:** XRD patterns for PPW precursors.

Analysts who worked on X-ray diffractogram investigations of activated carbons concluded that overwhelmingly amorphous solids have an expansive inner surface zone and pore volume. The effects of activation time on pore development, specific surface area, and pore volume of the prepared activated carbon were evaluated through Brunauer–Emmett–Teller (BET) and N<sub>2</sub> adsorption testing measured using Micromeritics TriStar II Plus (USA). Table 4 shows the BET surface area of activated carbon prepared from potato peel waste for AC precursors and products of both methods. In the present study, using KOH and CO<sub>2</sub>, most surface areas were greater than 800 m<sup>2</sup>/g, which is comparable to commercial activated carbon [21].

**Table 4:** Characteristics of potato peel waste (PPW) along with the ACs (PPCs and PPKs).

Samples		PPW1	PPW2	PPW3	PPC1	PPC2	PPC3	PPK1	PPK2	PPK3
BET results	SBET(m <sup>2</sup> /g)	1.8	2.4	775	775	1210	886	544	966	665
	Pore volume (cm <sup>3</sup> /g)	0.019	0.041	0.22	0.22	0.37	0.26	0.2	0.34	0.29

In previous studies, the pore development process through the activation process was analyzed. At a temperature of 1000°C, it was found to be 30.4% by XRD analysis [22]. In the present study, changes in the structural parameters (based on the XRD results) during the activation process were analyzed within the same stage classification as used in the previous study. Table 5 shows the degree of crystallinity within the enacted carbon powder. Figures 5-6 show that the AC-PPK with a KOH impregnation period of 24 h has a percent crystallinity is 35.03%, and the amorphous is 64.97% for PPK2, while the AC-PPC with a CO<sub>2</sub> activation period of 1 hour has a crystallinity of 35.46% with amorphous 64.54%. The reason that such an immoderate activation led to a decrease in the particle size and an increase in the degree of crystallinity was considered to be due to the movement of the carbon atoms and the reordering of the lattice layers. In all other cases, AC treated with KOHCO<sub>2</sub> appeared to have less crystallinity, which implies that the tests are semi-crystalline or undefined. In the case of enacted carbon, a few analysts detailed enacted carbon as being a shapeless material. Enacted carbon, which is generally regarded

as a shapeless carbon, has a large surface region and porosity. Previous studies have shown that the synthesized activated carbon is in a highly amorphous state of 64.8% and a low crystallinity of 35.2%, the results achieved in this study as agree with previous studies [23-25].

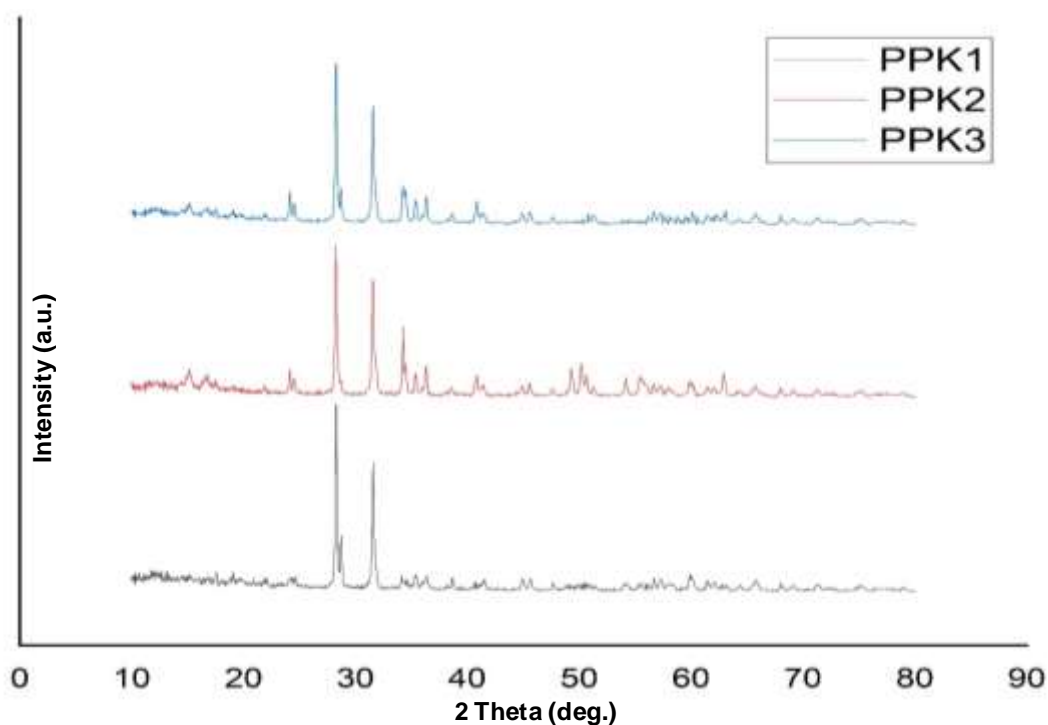


**Figure 5:** XRD patterns for chemical activation with KOH.

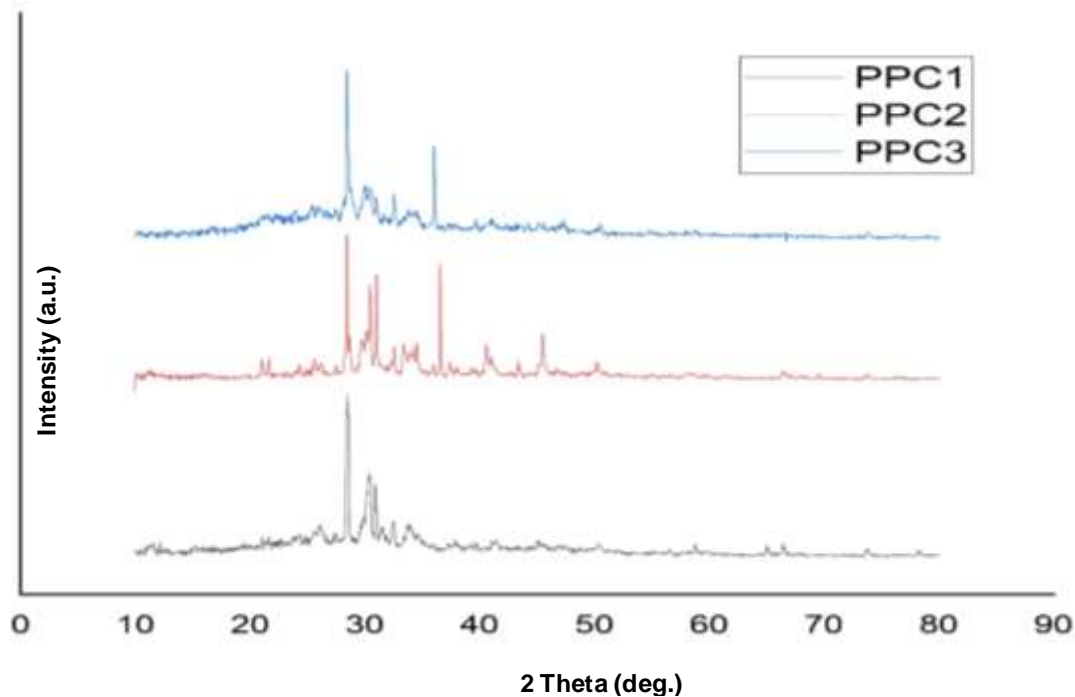


**Figure 6:** XRD patterns for Physical activation with CO<sub>2</sub>.

**Table 5:** Variation of percentage crystallinity of the AC.

Samples	AC by KOH, %	Samples	AC by CO <sub>2</sub> , %
PPK1	24.87	PPC1	18.76
PPK2	35.03	PPC2	35.46
PPK3	27.73	PPC3	19.18

The results of AFM analysis on the surface of the precursor PPWs are shown in Figures 7 (a–c), which depict a three-dimensional picture of the potato peel waste. It can be shown from these figures' numerous acute projections, the most noteworthy of which might reach up to 23 nm, 82 nm, and 29 nm with a scanning area of 1.00 μm x 1.00 μm. The enhancement within the drying period can be related to the surface morphology of the AC observed within the AFM picture, as shown in Figures 8 and 9, respectively. Which gives a high-elevation surface region for the carbon at 1396 nm (chemical activation) and 778 nm (physical activation) within a scanning area of 5.00 μm x 5.00 μm.

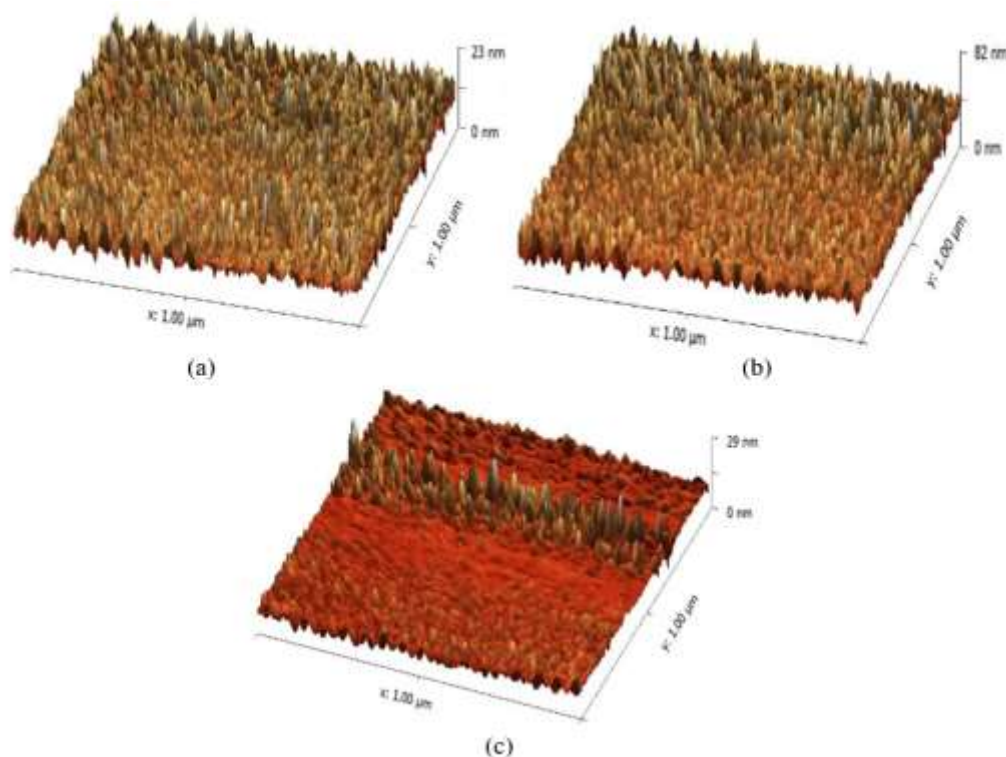


**Figure 7:** AFM at a magnification (1.00 μm x 1.00 μm) of precursor under the environment atmosphere (a) PPW1, (b) PPW2, and (c) PPW3

The surface morphology of precursor PPW, activated carbon PPK, and PPC was characterized using a FE-SEM test. Figures. 10 (a-c) refers to the nanostructure image for drying at 100°C within 12, 24, and 48 h, respectively. SEM macrographs Figures 11(a) and 12(a) show the external morphology of activated carbon by KOH activation via a chemical process under an atmosphere environment with a carbonization temperature of 500 °C and more intact compared to other activated carbons. The surface of the samples was found to be relatively organized without any pores except for some occasional cracks as compared to raw materials [13]. There are many clear, fine pores visible within the microstructure of activated carbon. The SEM pictures of the two activated carbons, PPK and PPC, indicated that the outside surfaces of these carbons were full of cavities and very unpredictable as a result of activation. There are many cracks, various splits, and small pits distributed over the surface, as well as little cavities dispersed over the surface, showing the extreme interaction of the KOH and CO<sub>2</sub> with PPW, which explains the difference between raw materials from agricultural wastes in previous studies [26, 27].

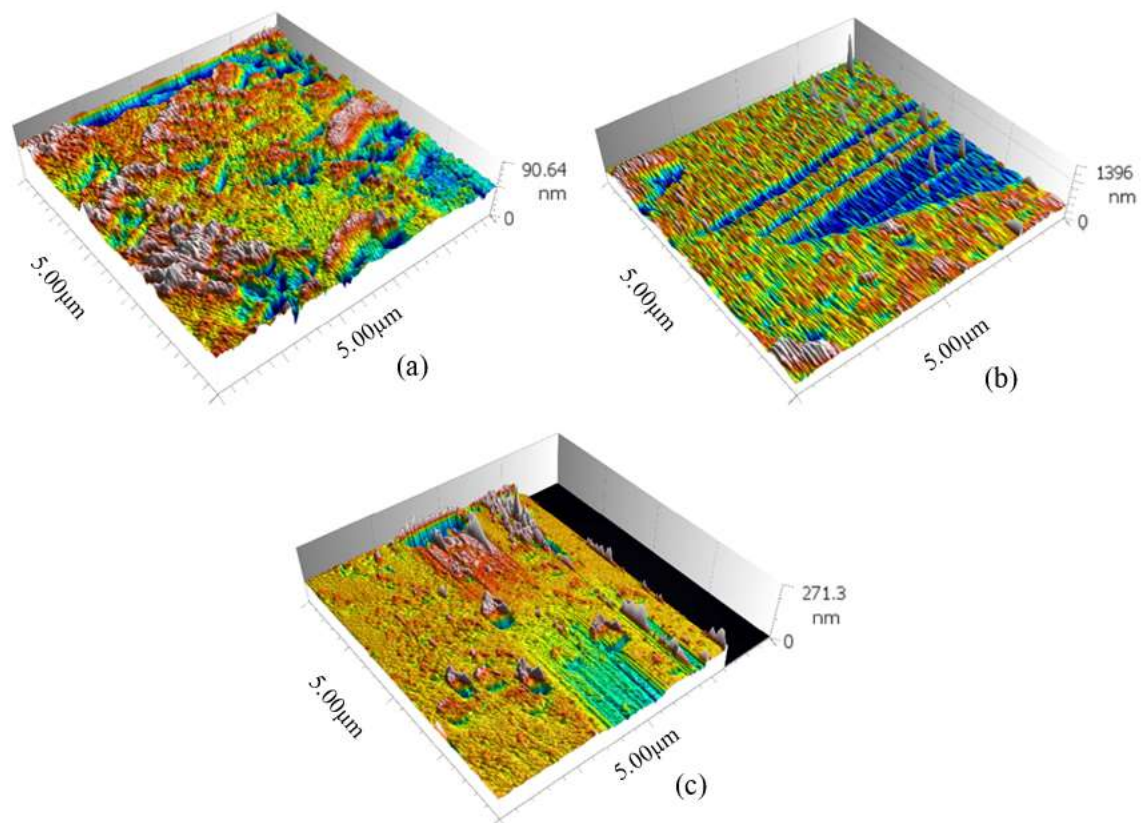


**Figure 8:** AFM at a magnification ( $5.00 \mu\text{m} \times 5.00 \mu\text{m}$ ) of precursor after chemical activation (a) PPK1, (b) PPK2, and (c) PPK3.

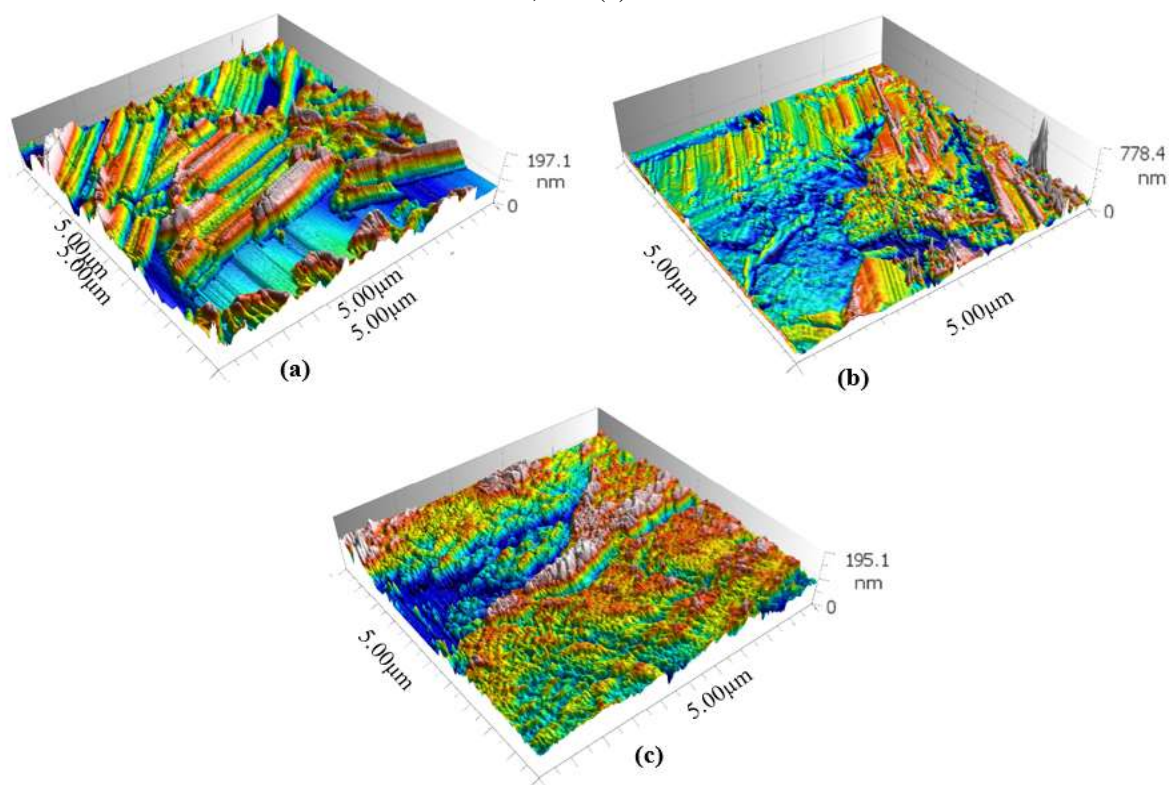


**Figure 9:** AFM at a magnification ( $5.00 \mu\text{m} \times 5.00 \mu\text{m}$ ) of precursor after chemical activation (a) PPC1, (b) PPC2, and (c) PPC3.



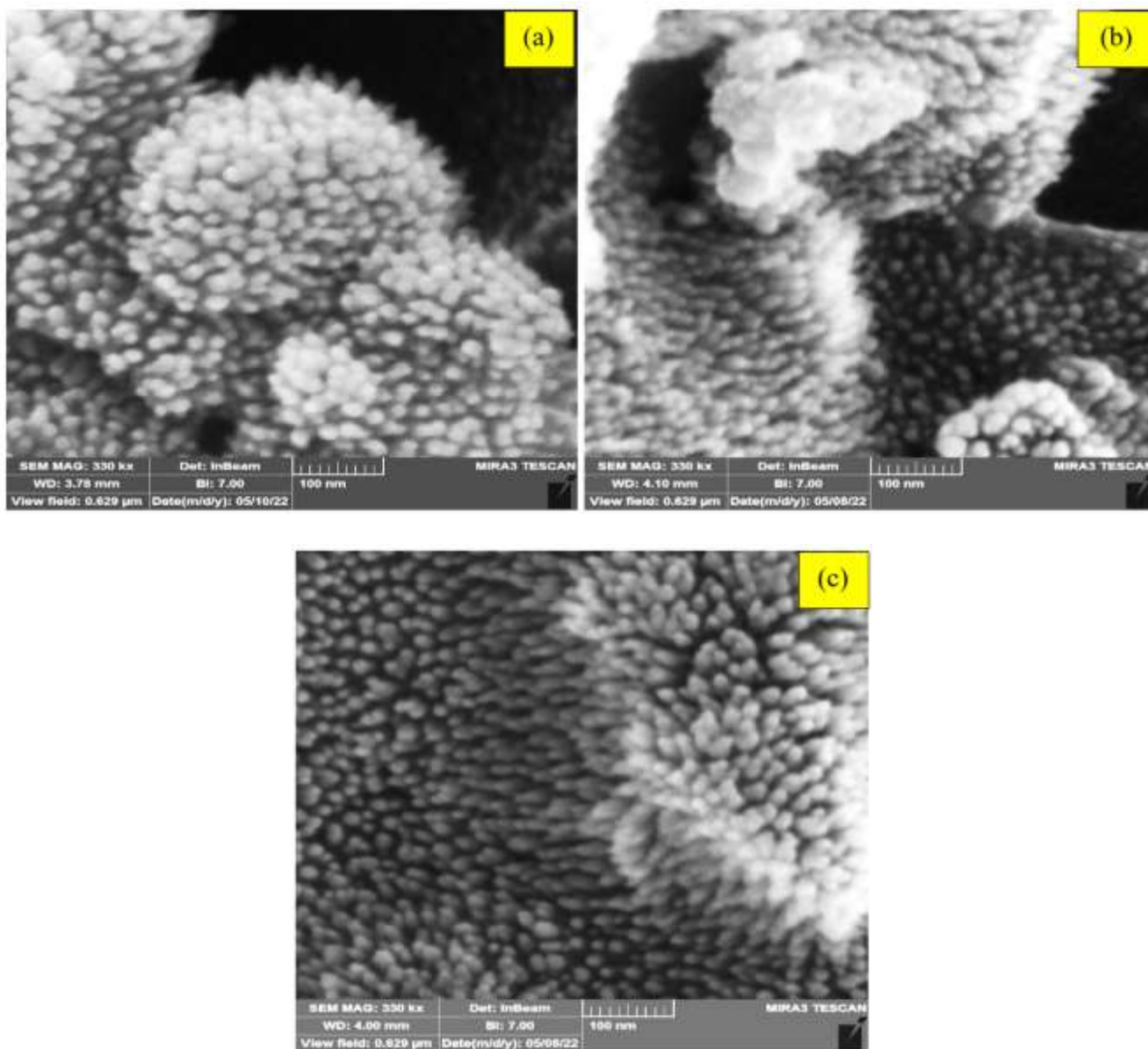


**Figure 10:** SEM at a magnification ( $1 \times 10.00kx$ ) of precursor under the environment atmosphere (a) PPW1, (b) PPW2, and (c) PPW3.

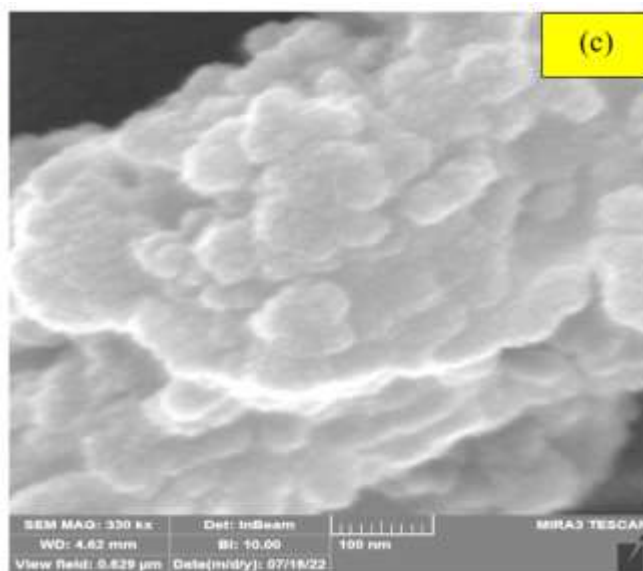
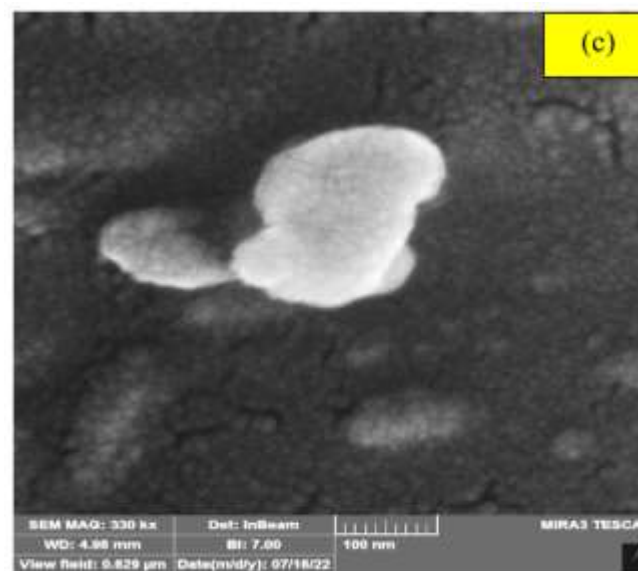
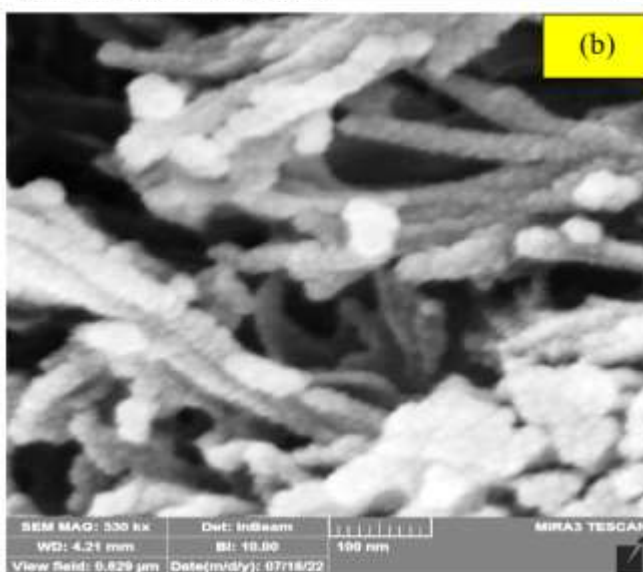
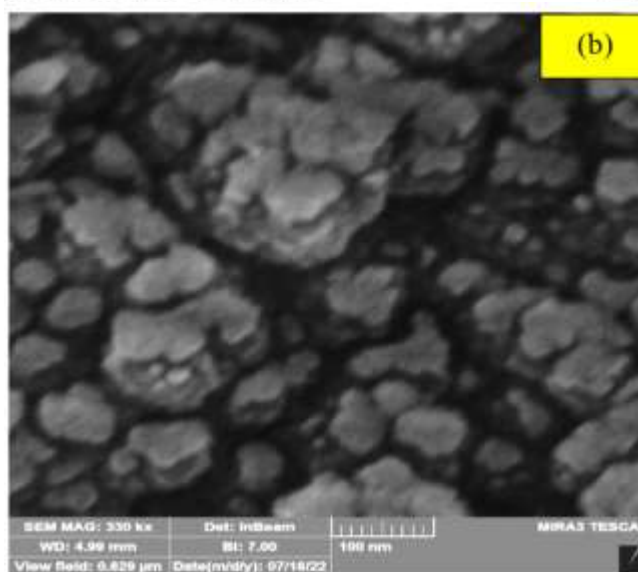
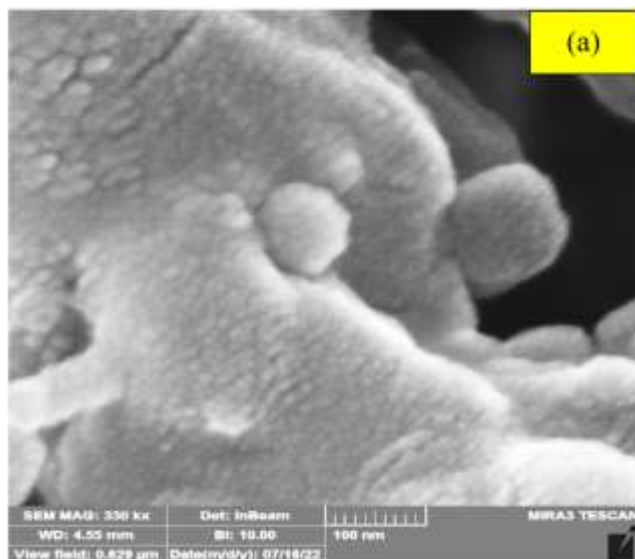
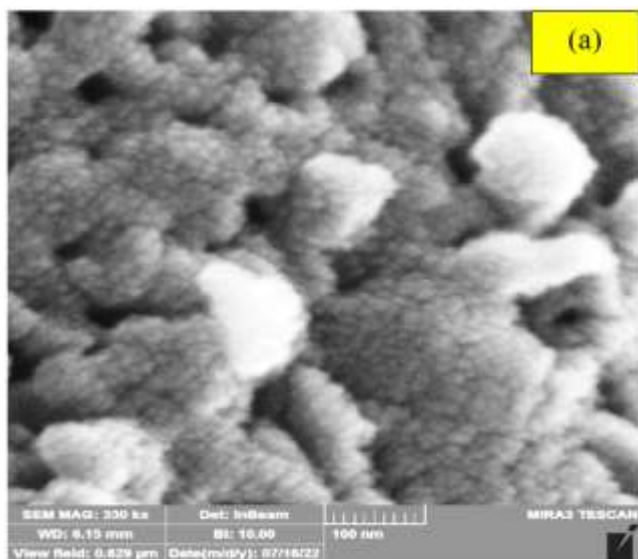


**Figure 11:** SEM at a magnification ( $1 \times 25.0 \text{KX}$ ) of precursor after chemical activation (a) PPK1, (b) PPK2, and (c) PPK3

**Figure 12:** SEM at a magnification ( $1 \times 25.0 \text{kx}$ ) of precursor after physical activation (a) PPC1, (b) PPC2, and (c) PPC3

#### 4. Conclusions

Activated carbon adsorbents have numerous applications and have changed applications in later times. Typically, the result of both a well-designed polydisperse permeable structure with a high degree of dispersion for atomic sorption and an expansive inside surface zone.

The AFM image of AC shows the presence of nanotips on the surface. PPK and PPC XRD results confirmed that the pore structure and lack of peak appearance were consistent. The XRD results confirmed that AC-treated KOH and CO<sub>2</sub> had a less crystalline appearance.

The activation of 3-FE-SEM-activated carbon photos derived from PPW by KOH is removed. Also, it appears that the outside surfaces of these carbons are full of cavities and very unpredictable as a result of being activated. This has been affirmed by the well-developed surface area that can be seen on the surface of the potato peel as it appears in this work.

Surface advancement within the potato peel amid pyrolysis was critical, as this would improve the surface area and pore volume of the PPK versus the PPC by accelerating the dissemination of KOH atoms into the pores and subsequently expanding the KOH carbon response through corrosive hydrolysis forms, which would then make more pores.

#### Acknowledgments

We are grateful to the Graduate Studies Laboratory at the Department of Applied Sciences at the University of Technology for their assistance in activating the labs and providing us with the protocol for conducting these tests.

#### Conflict of Interest

The authors declare that they have no conflict of interest.

#### References

- [1] S. J. Park and K. D. Kim, "Influence of activation temperature on adsorption characteristics of activated carbon fiber composites," *Carbon*, vol. 39, p. 1741, 2001.
- [2] Sudipta De and Alina Mariana Balu, "Biomass-Derived Porous Carbon Materials: Synthesis and Catalytic Applications." *ChemCatChem*, vol.7, p. 1608-1629, 2015.
- [3] Salah M. El- Hagggar, "Sustainable Industrial Design and Waste Management," *PhD*, 2007.
- [4] Hongjing Fu, WojciechPikus, Wahida Zaman, et al, "Water Environment," *Research*, vol. 80, p. 1340-1396, 2008.
- [5] C. Ripp and M. Borck, in *Encyclopedia of Electrochemical Power Sources*, 2009.
- [6] Omkar S. Nille and Anil H. Gore, "Valorization of Agri-Food Wastes and By-Products," *Academic Press*, 2021.
- [7] José Luís Figueiredo and Manuel Fernando R. Pereira, "Novel Carbon Materials for CO<sub>2</sub> Adsorption", *Novel Carbon Adsorbents*, 2012.
- [8] Al-Hashimi, O., Hashim, K., Loffill, E., et al, "A comprehensive review for groundwater contamination and remediation: occurrence, migration and adsorption modelling," *Molecules*, vol. 26, p. 5913, 2021.
- [9] Lim, W. C., Srinivasakannan, Balasubramanian et al., "Activation of palm shells by phosphoric acid impregnation for high yielding activated carbon," *Journal of Analytical and Applied Pyrolysis*, vol. 88, p. 181–186, 2010.
- [10] Ekpete, O., Marcus, A. and Osi, "Preparation and characterization of activated carbon obtained from plantain (*Musa paradisiaca*) fruit stem," *Journal of Chemistry*, p. 1–6, 2017.
- [11] Zhang L, Candelaria SL, Tian J, Li Y, et al, "Copper nanocrystal-modified activated carbon for supercapacitors with enhanced volumetric energy and power density", *Journal of Power Sources*, 2013.
- [12] Salmani H., "A comparative study of copper (ii) removal on iron oxide, aluminum oxide and activated carbon by continuous down flow method", *Journal of Toxicology and Environmental Health Sciences*, 2013.
- [13] Ahmed I. Osman, Jacob Blewitt, Jehad K. Abu-Dahrieh, et al, "Production and characterization of activated carbon and carbon nanotubes from potato peel waste and their application in heavy metal removal", *Environmental Science and Pollution Research*, 2019.

- [14] Noor. Q. A. Hussan, Ali A. Taha and Duha S. Ahmed, “Characterization of Treated Multi-Walled Carbon Nanotubes and Antibacterial Properties”, *Journal of Applied Sciences and Nanotechnology*, vol. 1, 2021.
- [15] Ibsa Nemea, Girma Gonfa and Chandran Masibc, “Activated carbon from biomass precursors using phosphoric acid”, *Heliyon*, 2022.
- [16] Chantakorn Patawat, a Ketsara Silakate and A Somchai Chuan-Udom, “Preparation of activated carbon from *Dipterocarpus alatus* fruit and its application for methylene blue adsorption”, *The Royal Society of Chemistry*, 2020.
- [17] Jon Alvarez, Gartzzen Lopez, Maider Amutio et al, “Physical Activation of Rice Husk Pyrolysis Char for the Production of High Surface Area Activated Carbons”, *Industrial & Engineering Chemistry Research*, 2015.
- [18] Junaid Saleem, Junaid Saleem, Usman Bin Shahid et al, “Production and applications of activated carbons as adsorbents from olive stones”, *Biomass Conversion and Biorefinery*, 2019.
- [19] Hernández-Montoya V, García-Servin J and Bueno-López JI, “Thermal Treatments and Activation Procedures Used in the Preparation of Activated Carbons”, *Journal of the Air & Waste Management Association*, 2012
- [20] D. G. Chukhchin, A. V. Malkov, I. V. Tyshkunova, et al, “Diffractometric Method for Determining the Degree of Crystallinity of Materials”, *Crystallography Reports*, 2016.
- [21] M. Ahmedna, W. E. Marshall, and R. M. Rao, “Production of granular activated carbons from select agricultural by products and evaluation of their physical, chemical, and adsorptive properties”, *Bioresource Technol. Bioresource Technol*, 2000.
- [22] Sang-Min Lee, Sang-Hye Lee and Jae-Seung Roh, “Analysis of Activation Process of Carbon Black Based on Structural Parameters Obtained by XRD Analysis”, *Crystals*, 2021.
- [23] Kamegawa, K., Nishikubo, K., and Yoshida, H., “Oxidative degradation of carbon blacks with nitric acid (I)—Changes in pore and crystallographic structures”, *Carbon*, p. 433–441, 1998.
- [24] Sharma, A., Kyotani, T., and Tomita, A., “A new quantitative approach for microstructural analysis of coal char using HRTEM images”, *Fuel*, p. 1203–1212. 1999.
- [25] D. Das, D. P. Samal, B. C. Meikap, Preparation of activated carbon from green coconut shell”, *J. Chem. Eng. Process Technol.*, p.1-7, 2015
- [26] Kang D. S., Lee S. M., Lee, S. H et al., “X-ray diffraction analysis of the crystallinity of phenolic resin-derived carbon as a function of the heating rate during the carbonization process”, *Carbon Lett.*, 2018.
- [27] Abdel-Nasser A.El-Hendawy, Andrew J.Alexander, Robert J.Andrews, et al, “Effects of activation schemes on porous, surface and thermal properties of activated carbons prepared from cotton stalks”, *Journal of Analytical and Applied Pyrolysis*, p. 272-278, 2008.